私立東海大學資訊工程與科學研究所

碩士論文

指導教授：林祝興 博士

Dr. Chu-Hsing Lin

全頻域浮水印技術強韌性之研究

A Study on the Robustness of Full-Band Watermarking Technologies

研究生：韓培真

(Pei-Chen Han)

中 華 民 國 九 十 七 年 六 月

博碩士論文電子檔案上網授權書

本授權書所授權之論文為授權人在 東海大學 資訊工程與科學系 ________組 96 學年度第 二 學期取得 碩士 學位之論文。

論文題目： 全頻域浮水印技術強韌性之研究

指導教授： 林祝興 劉榮春

茲同意將授權人擁有著作權之上列論文全文（含摘要），非專屬、無償授權國家圖書館及本人畢業學校圖書館，不限地域、時間與次數，以微縮、光碟或其他各種數位化方式將上列論文重製，並得將數位化之上列論文及論文電子檔以上載網路方式，提供讀者基於個人非營利性質之線上檢索、閱覽、下載或列印。

- 讀者基非營利性質之線上檢索、閱覽、下載或列印上列論文，應依著作權法相關規定辦理。

授權人：韓培真

簽　名：韓培真

中華民國 97 年 07 月 16 日

東海大學碩士學位論文考試審定書

東海大學資訊工程與科學系 研究所

研究生 韓 培 真 所提之論文

全頻域浮水印技術強韌性之研究

經本委員會審查，符合碩士學位論文標準。

學位考試委員會
召 集 人 ______________________ 簽章

委 員 ______________________

____

____

指 導 教 授 ______________________ 簽章

中華民國 97 年 6 月 27 日

Abstract

Internet has become indispensable of our lives; most of multimedia materials are digitally stored. Multimedia images, video and audio are digitalized and distributed expediently through the Internet. Unauthorized reproduction and distribution of digital multimedia files infringe the intellectual rights of art creators. Therefore, in the opening Internet world, protection of copyrights of digital content is getting more and more important. Digital world needs a good watermarking scheme which is immune to all kinds of attacks. Full-Band Image Watermarking (FBIW) scheme transforms original image data from the spatial domain into the frequency domain by using multi-scale Distributed Discrete Wavelet Transformation (DDWT), and then embeds watermarks in the four sub-bands: LL_3 & HH_3 by the DDWT watermarking method, LH_3, HL_3 by the Singular Value Decomposition (SVD) watermarking method. In this thesis, we investigate the security of the FBIW scheme by launching a variety of attacks and demonstrate experimentally that the FBIW technique is robust against image attacks. Experimental results show that FBIW is not only robust against most image attacks, such as rotation, cropping, the ripple, and the whirlpool attacks, but also robust against creative and multiple image attacks, such as the kaleidoscope plus tile, the kaleidoscope plus puzzle, and the kaleidoscope plus tile and puzzle attacks. We also investigate the influence of embedding watermark information in different layers of color image, i.e. the RGB layers. A second form of FBIW that embeds watermarks in sub-bands LH_3 & HL_3 by the DDWT, and LL_3, HH_3 by the SVD methods is studied, too. Stego-images processed by the second form of the FBIW method are shown to be slightly more robust than the first form.

Keywords：SVD, DDWT, Full-band image watermarking, Information hiding, Digital watermark, Copyright protection, Image attack

摘要

數位生活與網路應用，密不可分。多媒體資料，多以數位化來做存取。多媒體影像、影帶、音訊經數位化後，經由網路快速傳播。如果數位多媒體檔案，被未經授權地再製和散佈，將會侵犯了智慧財產權的擁有人的權利；所以，在網路的世界中，數位版權內容的保護日形重要，可以防患大多數影像攻擊的浮水印技術，成為數位生活的關鍵科技。全頻率域影像浮水印(Full-Band Image Watermarking, FBIW) 將原始影像的資料，藉由多重的分佈式離散小波轉換，從空間域轉換至頻率域，再嵌入浮水印資訊至四個頻率域：將浮水印，藉由分佈式離散小波轉換，嵌入至 LL_3 與 HH_3 頻率域；及藉由奇異值分解，嵌入至 LH_3 與 HL_3 頻率域。本論文經由多樣化的影像攻擊類型，深入探討 FBIW 浮水印技術的安全性。實驗證明 FBIW 技術，對於影像攻擊具有相當的強韌性。實驗結果驗證了 FBIW 不僅可以對抗大多數常見的影像攻擊，例如：旋轉、裁切、水波和漩渦等；也能夠抵抗創意性與多重的影像攻擊，例如：萬花筒加磚塊、萬花筒加拼圖，以及萬花筒加磚塊加拼圖等。本文亦研究了浮水印嵌入在不同色層〔RGB 色層〕造成的影響，以及探討了第二型態的 FBIW 技術：將浮水印，藉由分佈式離散小波轉換，嵌入在 LH_3 與 HL_3 頻率域，及藉由奇異值分解，嵌入在 LL_3 與 HH_3 頻率域。實驗結果亦驗證了第二型態的 FBIW 浮水印嵌入技術，比第一型態的 FBIW 浮水印嵌入技術，更具強韌性。

Keywords：奇異值分解，分佈式離散小波轉換，全頻率域影像浮水印，資訊隱藏，數位浮水印，版權保護，影像攻擊

致 謝

首先誠摯的感謝指導教授林祝興博士及劉榮春博士，兩位老師悉心的教導使我得以一窺資訊安全領域的深奧，不時的討論並指點我正確的方向，使我在這些年中獲益匪淺。老師對學問的嚴謹更是我輩學習的典範。

本論文的完成另外亦得感謝靜宜大學的翁永昌教授、羅峻旗教授及胡育誠教授為我在大學時期奠定下良好的基礎。因為有你們的體諒及幫忙，使得本論文能夠更完整而嚴謹。

兩年裡的日子，實驗室裡共同的生活點滴，學術上的討論、言不及義的閒扯、讓人又愛又怕的宵夜、趕作業的革命情感、因為睡太晚而遮遮掩掩閃進實驗室........，感謝眾位學長姐、同學、學弟妹的共同砥礪，你/妳們的陪伴讓兩年的研究生活變得絢麗多彩。

感謝鎮宇、建鑫學長、麗靜、宛如學姐們對於我研究指教評點，且總能在我迷惘時為我解惑，也感謝盈伶、依婷、念慈、幸儒、郁青、嘉文等同學的支持，以及昌明、采倫、文生、聖川、品仁、小拉的力挺，更謝謝明曦以及幼幼班朋友們的鼓勵。

母親在背後的默默支持更是我前進的動力，沒有的體諒、包容，相信這兩年的生活將是很不一樣的光景。

最後，謹以此文獻給我摯愛的母親－姚台鳳

韓培真　謹上 2008/7

Contents

Figures

Tables

Chapter 1
Introduction

Internet has become indispensable of our lives; it has been used for communications, file transfer, e-shopping, and entertainments, etc. Multimedia images, video and audio are digitalized and distributed expediently through the Internet. Unauthorized reproduction and distribution of digital multimedia files infringe the intellectual rights of art creators. For protection of rightful owners, many digital watermarking schemes as well as digital fingerprinting techniques have been developed.

Violations of intellectual property rights are rampant nowadays. Protection of copyrights of digital content is getting more and more important. Digital watermarking can effectively protect the rightful owners' intellectual property rights. Watermark information is embedded into digital media by their owners, and if the digital media are duplicated or used without suitable authorization, the watermark information can be extracted from the digital media by the owners as evidences of the ownership [13, 23].

Digital watermark techniques are divided into two types: visible and invisible watermarks. The visible watermark jeopardizes the image quality and is easily recovered by image processing; therefore, it is seldom applied in commercials. The invisible watermark has advantage of hiding copyright information without causing vast changes in the cover image. Compared with the visible watermarking technique, invisible watermarking technique is more valuable in protecting digital intellectual rights.

Effective watermarking schemes embed watermarks invisibly in original cover images and must be robust against image processing attacks [4, 14]. New techniques of image attacks evolve along with the development of image processing tools and they present great menace to digital watermarking schemes [11]. In 2006, Lin et al. proposed a Full-Band Image Watermarking (FBIW) scheme [2, 12] that is robust against most geometric and non-geometric attacks. In this thesis, we investigate the security of the FBIW scheme by launching a variety of attacks; some of them modify or distort the watermark images, or the stego-images, the others creatively manipulate the stego-images to produce new pieces of artwork. The experimental results show that the FBIW scheme is robust against all of the above mentioned attacks.

Digital world needs a good watermarking scheme which is immune to all kinds of attacks. Many related articles propose watermarking techniques without demonstrations of their robustness under variety of attacks. This thesis demonstrates experimentally that the Full-band image watermarking technique is robust against image attacks [9].

The rest of this thesis is organized as follows. In Chapter 2, the background of related techniques is briefly reviewed and the multi-scale FBIW scheme is described. Experimental results are shown in Chapter 3. In Chapter 4, we improve our watermarking method by considering a second form of FBIW. We then conclude the thesis in Chapter 5.

Chapter 2
PRELIMINARIES

The FBIW watermarking scheme combines the Distributed Discrete Wavelet Transformation (DDWT) watermarking scheme and the Singular Value Decomposition (SVD) watermarking scheme.

2.1 Lin's Distributed Discrete Wavelet Transformation Scheme (DDWT)

We will address the DDWT watermarking scheme in this section.

The DDWT watermarking scheme belongs to frequency domain watermarking techniques, which first transform data of the original image or media from the time domain into the frequency domain, and then embed the watermark information into the image or media in the transformed domain. Comparing with spatial domain watermarking techniques, frequency domain watermarking techniques are more capable to resist image attacks, that is, they are more robust.

The DDWT watermarking scheme is derived from the well-known Discrete Wavelet Transform (DWT). Based on the Continuous Wavelet Transform (CWT), there are many wavelet watermarking technologies. CWT spends too much of time and resources in the transforming process, DWT is preferred to solve this problem. In 1976, DWT was first proposed. According to the sub-band coding method, DWT is shown to be able to do wavelet transform with fast operations. After that, the wavelet technology is proven to be a new fundamental way on signal processing and is also called as sub-band coding technique. The advantage of DWT is that it can decrease the consumption of time and resources easily. Some researchers have used DWT to solve multi-resolution analysis or related problems. DWT is the most used in digital watermarking technology for intellectual property protection in recent year.

DWT has a variety of classes. Harr DWT is one of them; its scheme performs fast and is easy to implement. DDWT adopts the Harr DWT and improves its performance against attacks by means of a watermark embedding procedure proposed by Lin et al in 2006. DDWT watermarking can distribute watermark information uniformly in the spatial domain, whereas the watermark information is localized by using the DWT method. The aim of distributing information is to reduce the malicious depredations on the particular part of the image where the watermark information is centered. Imperceptibility and distribution of information are characteristics of DDWT watermarking; therefore this method is very robust against the cropping attack [10]. But this watermarking technology is not very robust against other geometric attacks such as rotation, scaling, and transposition or non-geometric attacks such as sharpening, blurring, and Gaussian noises.

2.2 Full-Band Image Watermarking (FBIW)

Based on the Discrete Wavelet Transform [1, 7, 15, 20, 25], Lin et al. proposed a Distributed Discrete Wavelet Transformation (DDWT) watermarking scheme [3] in 2006. The DDWT watermark scheme distributes hidden information in the spatial domain, so it works against localized destruction and improves the robustness of watermark. This technique is effective against many malicious attacks, especially the cropping attacks; but it is not good enough in the other geometric attacks, such as rotation, and resizing attacks.

The multi-scale DDWT transfers data in the spatial domain to the frequency domain, consisting of horizontal and vertical processes as follows [1, 6, 14]:

The horizontal process:

Step 1: Separate the original image along horizontal direction into two equal blocks.

Step 2: Add and subtract corresponding pixels on the two sub-blocks, then replace pixels on the left sub-block with the result of the addition and pixels on the right sub-block with the result of the subtraction. Denote the processed left sub-block as L and the right sub-block as H.

The vertical process:

Step 3: Separate the horizontally processed image along vertical direction into two equal blocks.

Step 4: Add and Subtract corresponding pixels on the two sub-blocks and replace pixels on the upper sub block with the result of the addition and pixels on the lower sub-block with the result of the subtraction. Thus, we generate four sub-blocks and denote them LL1, HL1, LH1 and HH1, which are the four band of the 1-scale DDWT. Repeat above horizontal and vertical processes on LL1 to obtain four band of the 2-scale DDWT and so on.

Fig. 1 shows the 1-scale DDWT. After applying the horizontal process on the original image S, sub-band L and H are obtained, and after applying the vertical process on L and H, the four sub-bands LL1, HL1, LH1 and HH1 are obtained. In order to get the 2-scale DDWT, we could take the sub-band LL1 and repeat step 1 to step 4. The original image generates seven bands from the result of the 2-scale DDWT. In the same way, the result of 3-scaled DDWT is obtained and shown in Fig. 2.

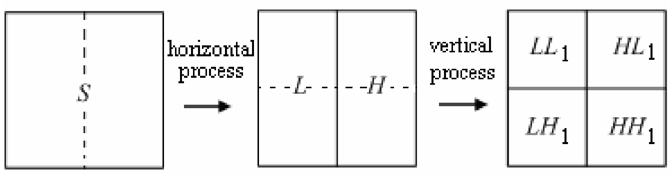

Figure 1. Block diagram of the 1-scale DDWT.

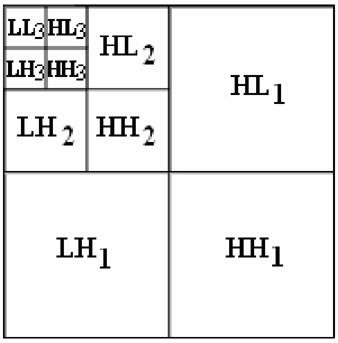

Figure 2. The result of the 3-scale DDWT

SVD was invented by Beltrami in 1873 to solve the square matrix problem. Eckart and Young improved it in 1930 and showed that a matrix can be approximated by another matrix of lower rank. Gene Golub proposed an algorithm that makes the computation of SVD feasible in 1970. Many researchers have since applied SVD at image compression [8, 9, 13, 21, 22, 24], watermarking [5, 6, 16, 25] and other signal processing fields [17, 18, 19, 23, 24].

SVD is a technique to unitarily diagonalize normal matrices by using a basis of eigenvectors. An image can be seen as a matrix composed of non-negative values.

For an image matrix $A \in R^{M \times N}$, where R is the real number and $M \geq N$, then

$$A = U \Sigma V^T = \sum_{i=1}^{m} \sigma_i u_i v_i^T \quad (1)$$

Where $U_{M\times M}$ and $V_{N\times N}$ are both orthogonal matrices and $\Sigma_{M\times N}$ is a diagonal matrix and m = min{M,N}. The scalars $\sigma_1, \sigma_2, \ldots, \sigma_m$ are the singular values of A. The vector u_i is the *i* column vector of matrix *U*. The vector v_i is the *i* column vector of matrix *V*. Each $u_i \times v_i^T$ is the basis matrix of matrix A.

2.3 Embedding and Extracting algorithm of FBIW

2.3.1 Embedding algorithm

Step 1: Input the original image *X* (*M*×*M*) and the watermark *W* (*N*×*N*).

Step 2: Perform the *K*-scale DDWT transform on *X* to obtain *X'*, where *K* is the number of scale.

(Step 3 to Step 6 embedding the watermark in *HL* and *LH* sub-bands utilizing the SVD method)

Step 3: Set initial values of the stego-image in the frequency domain Y' to be equal to X', and apply SVD on sub-bands *HL* and *LH* of the last scale:

$$\begin{aligned} X'^{HL} &= U_{X'}^{HL}\Sigma_{X'}^{HL}V_{X'}^{HLT} \\ X'^{LH} &= U_{X'}^{LH}\Sigma_{X'}^{LH}V_{X'}^{LHT} \end{aligned} \tag{2}$$

Where X'^{HL} and X'^{LH} represent X' in sub-bands *HL* and *LH*, and the diagonal elements ($\sigma_{X'i}^{HL}$ and $\sigma_{X'i}^{LH}$) of $\sum_{X'}^{HL}$ and $\sum_{X'}^{LH}$ are the singular values on sub-bands HL and LH. The singular values on sub-bands HL and LH must satisfy

$\sigma_{X'1}^{HL} \geq \sigma_{X'2}^{HL} \geq \cdots \geq \sigma_{X'M}^{HL} \geq 0$ and $\sigma_{X'1}^{LH} \geq \sigma_{X'2}^{LH} \geq \cdots \geq \sigma_{X'M}^{LH} \geq 0$.

Step 4: Apply SVD to the watermark:

$$W = U_W \Sigma_W V_W^T \tag{3}$$

Where the diagonal elements (σ_{Wi}) of Σ_W are the singular values of the watermark, and $\sigma_W = [\sigma_{W1}, \sigma_{W2}, \cdots, \sigma_{WN}]$, $\sigma_{W1} \geq \sigma_{W2} \geq \cdots \geq \sigma_{WN} \geq 0$

Step 5: Process the singular values of X' in the frequency domain with the singular values of the watermark:

$$\begin{aligned} \sigma_{Y_i}^{HL} &= \sigma_{X_i'}^{HL} + \alpha_i \sigma_{Wi} \\ \sigma_{Y_i}^{LH} &= \sigma_{X_i'}^{LH} + \alpha_i \sigma_{Wi} \end{aligned} \tag{4}$$

Where i=1, 2, ..., N and setting the value of α_i, α is a scaling factor. It will affect the quality of embedded watermark and $\sigma_{Y'}$ is the singular values of the singular matrix $\Sigma Y'$.

Step 6: Obtain Y'^{HL} and Y'^{LH} embedded with watermarks on sub-bands *HL* and *LH*:

$$Y^{HL} = U_{X'}^{HL} \Sigma_Y^{HL} V_{X'}^{HLT}$$
$$Y^{LH} = U_{X'}^{LH} \Sigma_Y^{LH} V_{X'}^{LHT} \quad (5)$$

Step 7: Take Y'^{HL} and Y'^{LH} of the last scale of Y' and perform inverse DDWT to obtain spatial domain Y_{HLLH} that has been embedded with watermarks in sub-bands *HL* and *LH*.

(Step 8 embedding the watermark in sub-bands *LL* and *HH* utilizing the DDWT method)

Step 8: Take Y' data in the sub-bands *LL* and *HH* of the last scale and embed watermark information according to the following formula:

$$\text{If } W_{ij} = 0 \text{ then } Y_{ij}^{LL} = Y_{ij}^{LL} + (2^K)^2 \times \alpha$$
$$\text{If } W_{ij} = 1 \text{ then } Y_{ij}^{HH} = Y_{ij}^{HH} + (2^K)^2 \times \alpha \quad (6)$$

Step 9: Apply the inverse DDWT to Y' to produce the stego-image Y, which has been embedded with watermark information on the four sub-bands of the last scale. Subtract Y_{HLLH} from Y to obtain Y_{Diff}, which gives difference of pixel values of Y_{HLLH} and Y in the spatial domain.

2.3.2 Extracting algorithm

(Step 1 to Step 2 extracting the watermark from sub-bands *LL* and *HH*)

Step 1: Input the stego-image Y, the original image X, the spatial domain data Y_{HLLH}, and the watermark W.

Step 2: Subtract Y_{HLLH} from Y to obtain Y_{LLHH}, and apply formula (7) on Y_{LLHH} to extract the embedded watermark W^{LLHH}:

$$W_{ij}^{LLHH} \begin{cases} = 0 & if\ E_{LLHH} < 0 \\ = 1 & otherwise \end{cases} \quad (7)$$

(Step 3 to Step 6 extracting the watermark from sub-bands *HL* and *LH*)

Step 3: Subtract Y_{Diff} from Y to obtain F, and then apply the multi-scale DDWT on F to obtain F'.

Step 4: Apply SVD to F' on sub-bands HL and LH of the last scale:

$$
\begin{aligned}
F'^{HL} &= U_{F'}^{HL} \Sigma_{F'}^{HL} V_{F'}^{HLT} \\
F'^{LH} &= U_{F'}^{LH} \Sigma_{F'}^{LH} V_{F'}^{LHT}
\end{aligned} \quad (8)
$$

Where F'^{HL} and F'^{LH} represent F' in the sub-bands HL and LH of the last scale, and the diagonal elements ($\sigma_{F'}^{HL}$ and $\sigma_{F'}^{LH}$) of $\sum_{F'}^{HL}$ and $\sum_{F'}^{LH}$ are the singular values of F'^{HL} and F'^{LH}.

Step 5: Extract the singular values of watermarks by processing the diagonal elements of $\sum_{F'}^{HL}$ with $\sum_{X'}^{HL}$ and $\sum_{F'}^{LH}$ with $\sum_{X'}^{LH}$, respectively.

$$
\begin{aligned}
\sigma_{W_i}^{HL} &= \frac{\sigma_{F_i'}^{HL} - \sigma_{X_i'}^{HL}}{\alpha_i} \\
\sigma_{W_i}^{LH} &= \frac{\sigma_{F_i'}^{LH} - \sigma_{X_i'}^{LH}}{\alpha_i}
\end{aligned} \quad (9)
$$

Where i = 1, 2… N. $\sigma_{W_i}^{HL}$ and $\sigma_{W_i}^{LH}$ is extracting SVD from HL and LH.

Step 6: Obtain the two watermarks embedded in sub-bands HL and LH by the following equations:

$$
\begin{aligned}
W^{HL} &= U_W^{HL} \Sigma_W^{HL} V_W^T \\
W^{LH} &= U_W^{LH} \Sigma_W^{LH} V_W^T
\end{aligned} \quad (10)
$$

2.4 Comparisons of FBIW, DDWT and DWT-SVD Methods

This research is a continuation of previous works in our laboratory. The related major historical results will be narrated in this section. Comparisons of the FBIW, the DDWT and the DWT-SVD method were made by Lin et al. In Kuo's thesis: A Robust Full-band Watermarking Scheme, experimental results of above three methods are summarized and are shown in Figure 5. It shows that the FBIW method is in general more robust than the DDWT and the DWT-SVD methods under all tested attacks.

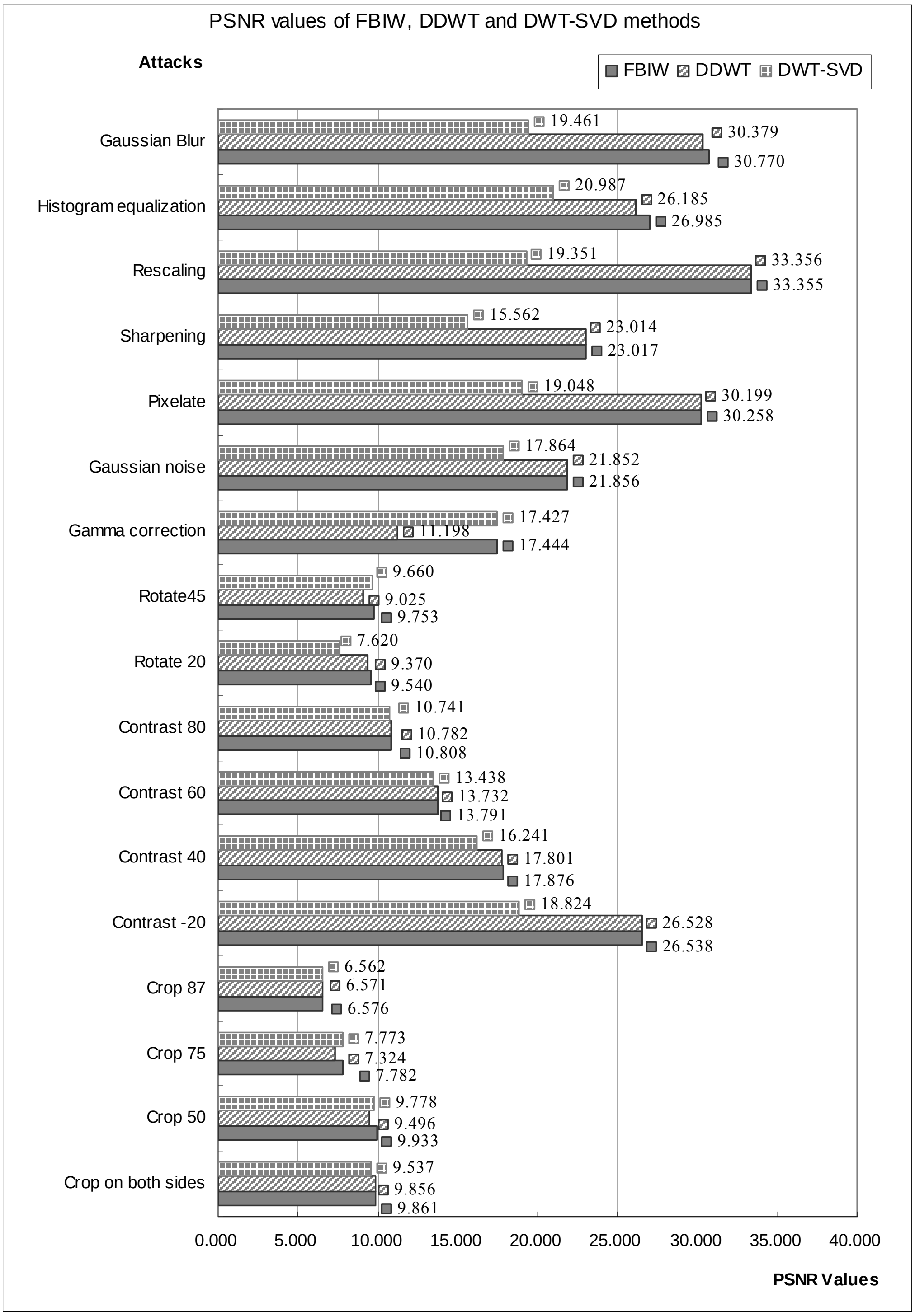

Fig. 3 PSNR values of the FBIW, DDWT and DWT-SVD methods
(Reprinted from "A Robust DDWT-SVD Image Watermarking Scheme")

Chapter 3

The experimental result of FBIW

The original cover image Lena (512 × 512) is shown in Fig. 3(a), and the watermark (64 × 64), in Fig. 3(b). The watermark, Tunghai Univerisy, is a masterpiece of calligraphy by the famous modern Chinese calligrapher Yu, You-ren (1879-1964). We embedded watermarks in the full band of the cover image after performing 3-scale DDWT on it. The scaling factor α of the watermark used in each sub-band is 1. The stego-image Lena is shown in fig. 4(a). The watermark is extracted from HH sub-band and LL sub-band in fig. 4(c) and fig. 4(d). The PSNR of FBIW method is 39.2793. If the image size is 1024*1024, the PSNR will be 43.3015. In the image attacks experiment, we adopt cover image with size of 512*512, which is more vulnerable to image attacks.

All the programs are implemented on a personal computer with Intel® Pentium M 735 CPU 1.70GHz, and 1.5 GB RAM, running Microsoft Windows XP® operating system. The programs are written in Visual C# programming language and MATLAB 7.0 programming language.

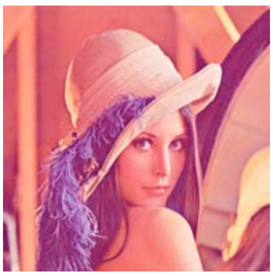

(a)

(b)

Fig. 4 (a) The original cover image of Lena (512×512) (b) The watermark (64×64).

(a) (b) (c) (d)

Fig. 5 (a) The stego-image of Lena (PSNR = 39.2793)
(b) Extracted watermarks embedded in sub-bands LL and HH
(c) The extracted watermark embedded in the sub-band HL
(d) The extracted watermark embedded in the sub-band LH.

To evaluate the robustness of watermarks, we use the Pearson Correlation Coefficient, which is a similarity measurement tool that judges the closeness between extracted watermark (W') and original watermark (W).

Pearson's Correlation Coefficient is used for measurement of correlation or association between the original watermark (W) and the extracted watermark (W′). The correlation coefficient ranges from −1 to 1. A value of 1 means that a linear equation describes the relationship perfectly and positively; a value of 0 indicate no correlation at all; a value of -1 indicates perfect negative correlation. We use the formula defined below:

$$Corr(W,W') = \frac{\sum_{i=0}^{n-1}\sum_{j=0}^{n-1}(W_{(i,j)} - \bar{W})(W'_{(i,j)} - \bar{W}')}{\sqrt{\sum_{i=0}^{n-1}\sum_{j=0}^{n-1}(W_{(i,j)} - \bar{W})^2}\sqrt{\sum_{i=0}^{n-1}\sum_{j=0}^{n-1}(W'_{(i,j)} - \bar{W}')^2}} \quad (11)$$

Where $\bar{W}$ and $\bar{W}'$, the average value of pixels of the original watermark and the extracted watermark respectively, are defined as follows:

$$\bar{W} = \frac{\sum_{i=0}^{n-1}\sum_{j=0}^{n-1}W_{(i,j)}}{n \times n}, \bar{W}' = \frac{\sum_{i=0}^{n-1}\sum_{j=0}^{n-1}W'_{(i,j)}}{n \times n} \quad (12)$$

The watermarked image, or the stego-image, is somewhat different from the cover image. To evaluate the fidelity of the stego-image, the peak signal-to-noise ratio (PSNR) was calculated as follows:

$$PSNR = 10\log\left(\frac{255^2}{MSE}\right) \qquad (13)$$

Where the mean square error (MSE) of the cover image (m×m) and the stego-image (m×m) is:

$$MSE = \frac{1}{m^2}\sum_{i=0}^{m-1}\sum_{j=0}^{m-1}(\alpha_{ij} - \beta_{ij})^2 \qquad (14)$$

Where α_{ij} is the pixel value of the cover image, and β_{ij} is the pixel value of the stego-image. The typical value of PSNR for lossy image is between 30 to 50 dB, and the higher, the better.

MSE is the Mean Square Error of the *m*×*m* images; α_{ij} is the pixel value at (i,j) before the encoding; β_{ij} is the pixel value at (*i,j*) after the encoding.

We launched varieties of attacks on the stego-image to investigate the robustness of the FBIW scheme. For the sake of space, we just list part of the experimental results with the most common attacks in the following sections.

3.1.1 Gaussian Noise Attack

We launched Gaussian attacks on the stego-image to investigate the robustness of the FBIW scheme which combines Distributed Discrete Wavelet Transformation and Singular Value Decomposition. For the sake of space, we just list part of the experimental results with the Gaussian noise attacks in Table 1.

Column 1 shows the sabotaged stego-images. Some of them are slightly modified by Gaussian noises with different parameter settings. Columns 2 to 4 show the extracted watermarks and their correlation coefficients. Since we have embedded watermarks in the full band: LH, HL, and LL&HH of the 3-scale DDWT, we can extract all of them from the attacked stego-image and use the best one for copyrights protections. The Pearson's correlation coefficients for the best extracted watermarks are greater than 0.5032 in Table 1. Considering the best extracted watermark of each attacking test, we find that the FBIW method is robust against Gaussian attacks.

Table 1 The best extracted watermarks and their Pearson's Correlation Coefficients after Gaussian Noise Attack

Gaussian Noise Attack	FBIW		
%	HL	LH	LL&HH
 5			
	0.7859	0.7858	0.0819
 10	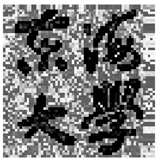	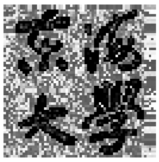	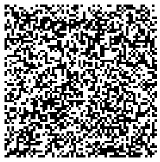
	0.6125	0.6039	0.0620
 20	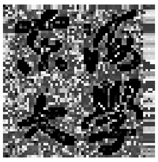	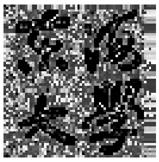	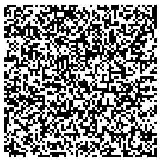
	0.5032	0.4930	0.0435

3.1.2 Contrast Attack

We investigated the robustness of the FBIW scheme against contrast attacks. The experimental results are listed in Table 2. The Pearson's correlation coefficients for the best extracted watermarks are greater than 0.7563. We find that the FBIW method is robust against contrast attacks.

Table 2 The best extracted watermarks and their Pearson's Correlation Coefficients after Contrast Attacks

Contrast Attack	FBIW		
Parameters (pixel)	HL	LH	LL&HH
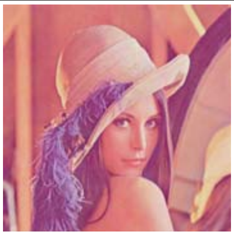 -20	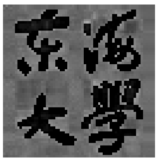	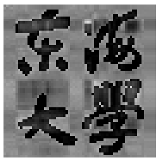	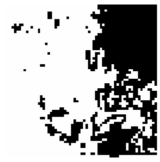
	0.7694	0.7094	0.3003
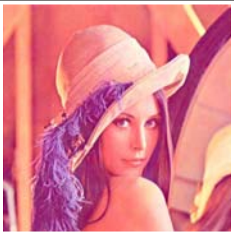 10	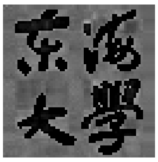	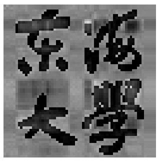	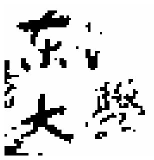
	0.8082	0.8053	0.6734
 20	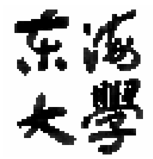	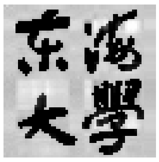	
	0.8166	0.8052	0.2825
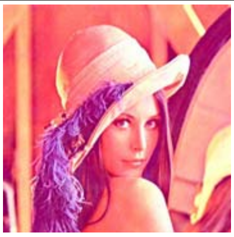 30	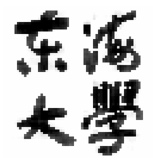		
	0.8253	0.8118	0.1894
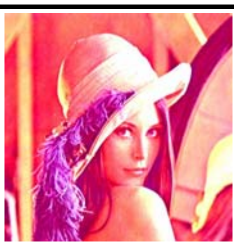 50	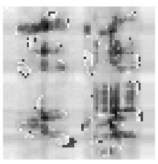	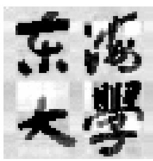	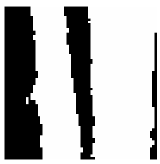
	0.6173	0.8083	0.1939
 80	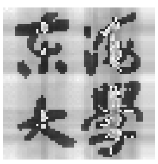	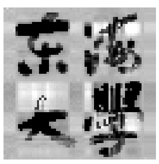	
	0.6325	0.7563	0.1982

3.1.3 Gaussian Blur Attack

We launched Gaussian blur attack on the stego-image to investigate the robustness of the FBIW scheme. The application software of Gaussian blur attack is PhotoImpact. The experimental results with the Gaussian blur attack are listed in Table 3. The Pearson's correlation coefficients for the best extracted watermarks are greater than 0.1336, which is not good numerically because that the Gaussian blur attack inverts the attributes of the embedded watermarks. But, we still can recognize the embedded watermarks by the eyes. So, we conclude that the FBIW method is robust against Gaussian blur attacks.

3.1.4 Sharpen Attack

We launched sharpen attack on the stego-image to investigate the robustness of the FBIW scheme. The application software of sharpen attack is PhotoImpact. The experimental results with the sharpen attack are listed in Table 4. The Pearson's correlation coefficients for the best extracted watermarks are greater than 0.8031. We conclude that the FBIW method is robust against sharpening attacks.

Table 3　The best extracted watermarks and their Pearson's Correlation Coefficients after Gaussian Blur Attacks

Gaussian Blur Attack	FBIW		
Radius (pixel)	HL	LH	LL&HH
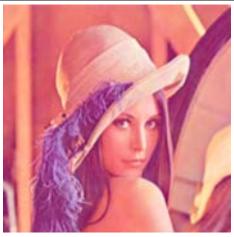	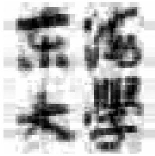	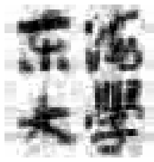	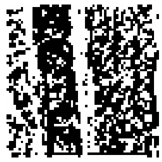
1	0.7843	0.7863	0.2324
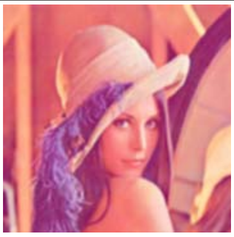	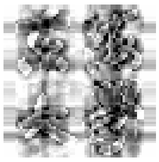	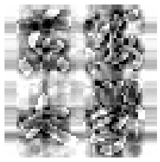	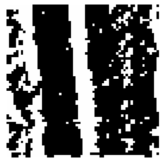
2	0.2883	0.2489	0.1458
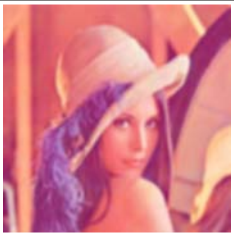	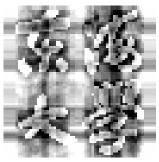	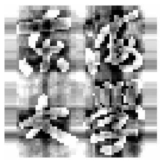	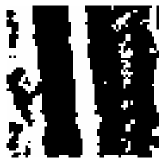
3	-0.0754	-0.1336	0.1452
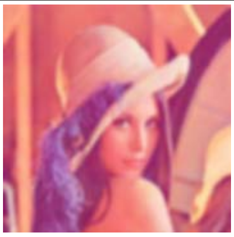	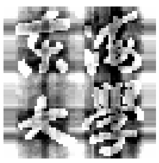	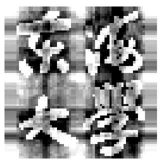	
4	-0.2930	-0.3399	0.1561
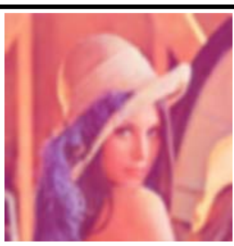	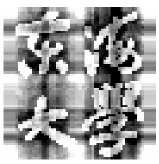	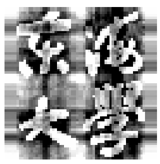	
5	-0.3430	-0.3869	0.1592

Table 4 The best extracted watermarks and their Pearson's Correlation Coefficients after Sharpen Attacks

Sharpen Attack			FBIW		
Amount (%)	Radius (pixels)	Threshold (levels)	HL	LH	LL&HH
 30, 10, 0			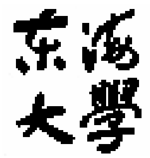	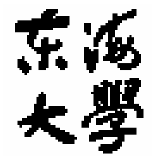	
			0.8032	0.8032	0.5615
 30, 20, 0			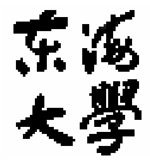	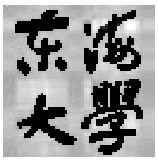	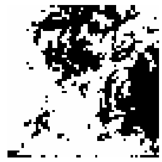
			0.8040	0.7971	0.3535
 30, 30, 0			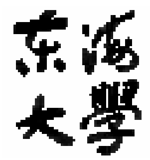	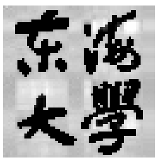	
			0.8127	0.7997	0.2935
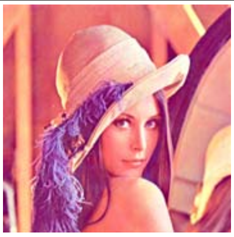 30,50, 0				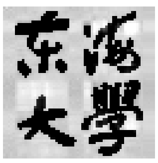	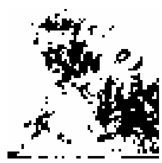
			0.8213	0.8027	0.3753
 30, 80, 0				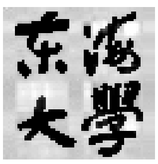	
			0.8220	0.8030	0.2898

3.1.5 Histogram equalization Attack

We launched histogram equalization attacks on the stego-image to investigate the robustness of the FBIW scheme. The application software of histogram equalization attacks is PhotoImpact. For the histogram equalization attack, we setup auto layer of PhotoImpact adjustment in color. We list the experimental results with the sharpen attack in Table 5. The Pearson's correlation coefficients for the best extracted watermarks are greater than 0.8163. We conclude that the FBIW method is robust against histogram equalization attacks.

Table 5 The best extracted watermarks and their Pearson's Correlation Coefficients after Histogram equalization Attacks

Histogram equalization Attack	FBIW		
	HL	LH	LL&HH
	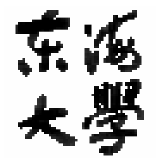	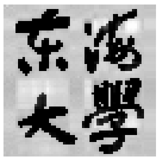	
	0.8164	0.8050	0.2143

3.1.6 Rotation Attack

We launched rotation attacks on the stego-image to investigate the robustness of the FBIW scheme. The application software of rotation attack is PhotoImpact. We list the experimental results with the rotation attacks in Table 6. The Pearson's correlation coefficients for the best extracted watermarks are greater than 0.9582. We conclude that the FBIW method is robust against rotation attacks.

Table 6 The best extracted watermarks and their Pearson's Correlation Coefficients after Rotation Attacks

Rotation Attack	FBIW		
angle	HL	LH	LL&HH
			
15°	0.8027	0.8029	0.9582
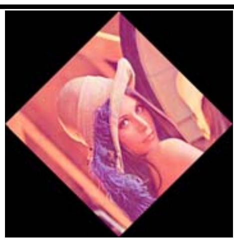			
45°	0.8027	0.8029	0.9582
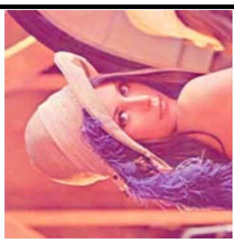			
90°	0.8027	0.8029	0.9582

3.1.7 Cropping Attack

We launched cropping attacks on the stego-image to investigate the robustness of the FBIW scheme. The application software of cropping attack is PhotoImpact. We list the experimental results with the cropping attacks in Table 7. The Pearson's correlation coefficients for the best extracted watermarks are greater than 0.9582. We conclude that the FBIW method is robust against cropping attacks.

Table 7 The best extracted watermarks and their Pearson's Correlation Coefficients after Cropping Attacks

Cropping Attack	FBIW		
area (%)	HL	LH	LL&HH
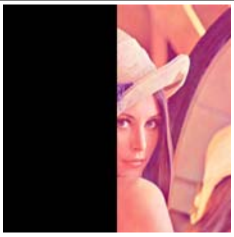 50%	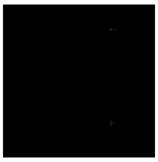		
	-0.0333	-0.6457	0.9582
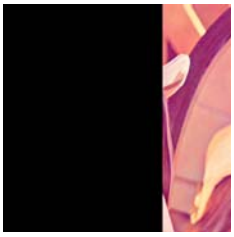 70%		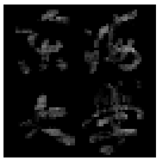	
	-0.1655	-0.6338	0.9582
 95%		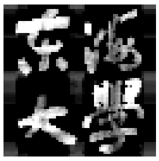	
	-0.3271	-0.7683	0.9582

3.1.8 Fills and Textures

We launched fill and textures attacks on the stego-image to investigate the robustness of the FBIW scheme. The application software of fill and textures attack is PhotoImpact. We list the experimental results of fill and textures attacks in Table 8. The Pearson's correlation coefficients for the best extracted watermarks are greater than 0.5068. We conclude that the FBIW method is robust against fill and textures attacks.

Table 8 The best extracted watermarks and their Pearson's Correlation Coefficients after Fills and Textures Attacks

Fills and Textures	FBIW		
	HL	LH	LL&HH
	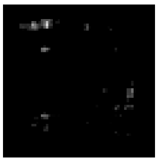	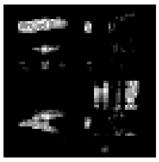	
Emboss: 1	-0.2875	-0.5388	0.2068
		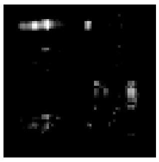	
Emboss: 5	-0.0859	-0.3108	0.2119
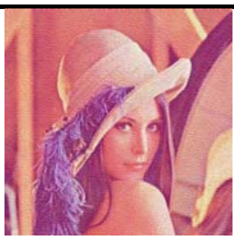	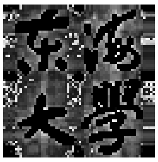	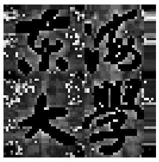	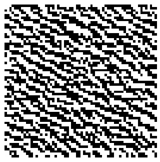
Texture Filter-Effect Embossed	0.5068	0.4837	0.0352

3.1.9 Lighting

We launched lighting attacks on the stego-image to investigate the robustness of the FBIW scheme. The application software of lighting attack is PhotoImpact. We list the experimental results with the lighting attacks in Table 9. The Pearson's correlation coefficients for the best extracted watermarks are greater than 0.7975. We conclude that the FBIW method is robust against lighting attacks.

Table 9 The best extracted watermarks and their Pearson's Correlation Coefficients after Lighting Attacks

Lighting Attack	FBIW		
	HL	LH	LL&HH
 Lighting		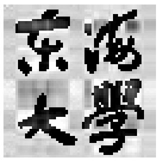	
	0.7975	0.7629	0.1646
 Cool-Blue:2			
	0.8027	0.8027	0
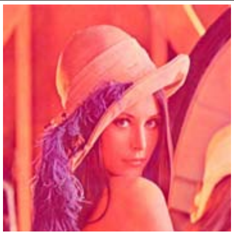 Warm-Red:2			
	0.8027	0.8027	0

3.1.10 Distort

We launched distort attacks on the stego-image to investigate the robustness of the FBIW scheme. The application software of distort attacks is PhotoImpact. We list the experimental results with the distort attacks in Table 10. The distort attacks include fat, thin, punch, ripple, whirlpool, crystal and glass, blast-lift, and stagger-lift. The Pearson's correlation coefficients for the best extracted watermarks are greater than 0.4556. We can find FBIW method after distort attack is robust from Table 10.

Table 10 The best extracted watermarks and their Pearson's Correlation Coefficients after Distort Attacks

Distort Attack	FBIW		
	HL	LH	LL&HH
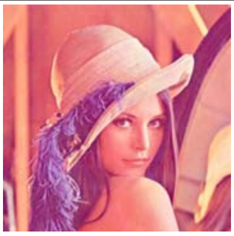 Fat: 3		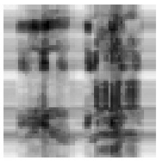	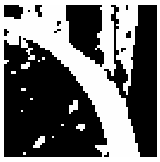
	0.5343	0.6677	0.2085
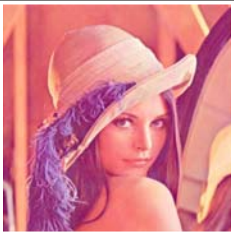 Fat: 5	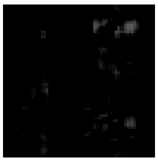	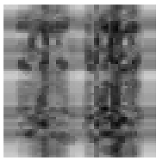	
	0.1008	0.5170	0.1697
 Thin: 3	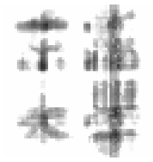	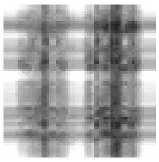	
	0.6920	0.4458	0.2212
 Thin: 5	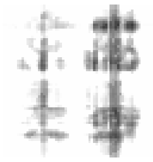	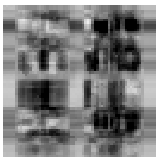	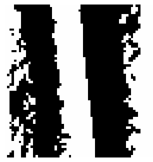
	0.4556	0.3346	0.2344
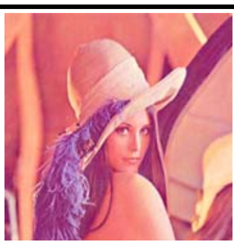 Pinch	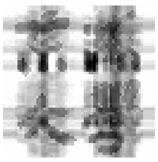	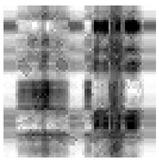	
	0.6293	0.2122	0.9582
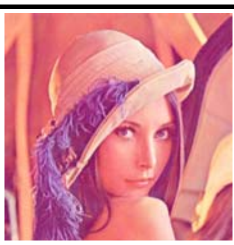 Punch	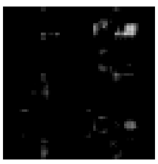	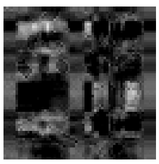	
	0.099	-0.1796	0.9582

 Ripple	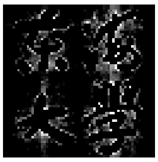	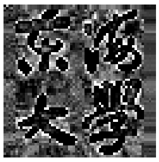	
	0.2229	0.4532	0.9582
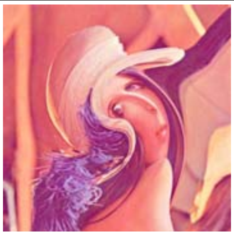 Whirlpool	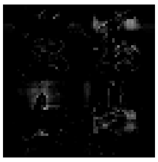		
	0.0877	-0.1175	0.9582
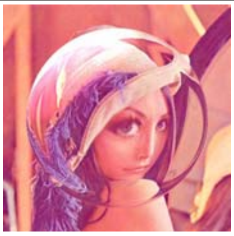 Crystal and Glass	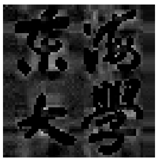	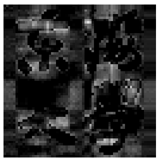	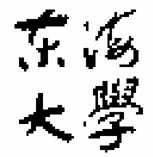
	0.5207	0.2118	0.9582
 Blast-Lift:60		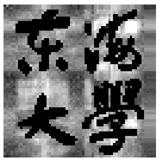	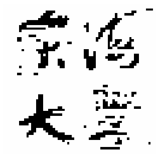
	0.7646	0.7037	0.7757
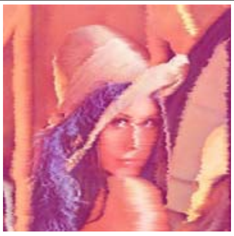 Stagger-Lift		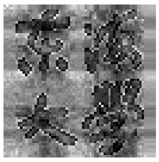	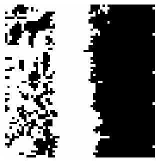
	0.6300	0.4955	0.1835

3.1.11 Artistic

We launched artistic attacks on the stego-image to investigate the robustness of the FBIW scheme. The application software of artistic attack is PhotoImpact. We list the experimental results with artistic attacks in Table 11. The Pearson's correlation coefficients for the best extracted watermarks are greater than 0.7241. We conclude that the FBIW method is robust against artistic attacks.

Table 11 The best extracted watermarks and their Pearson's Correlation Coefficients after Artistic Attacks

Artistic Attack	FBIW		
	HL	LH	LL&HH
 Watercolor-Little:80			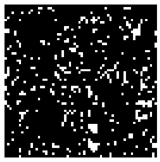
	0.8009	0.7879	0.1433
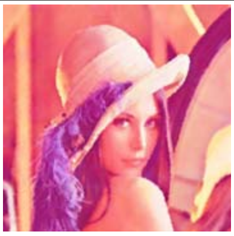 Oil Paint:5,50	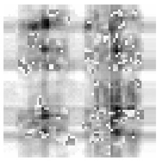	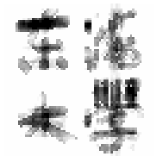	
	0.4671	0.7241	0.1788
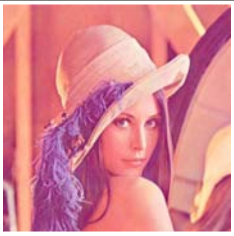 Colored Pen:5	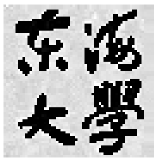		
	0.7990	0.7946	0.6108

3.1.12 Creative

Image processing tools are used not only to attack the watermarking information but also to reprocess the stego image in creative ways. Table 12 shows reprocessed images of Lena on PhotoImpact, but all of them have been disguised so much that one can hardly associate them with Lena at first glance. To one's surprise, the extracted watermarks are still very clear. The Pearson's correlation coefficients for the best extracted watermarks are greater than 0.5425. The experimental results show that the FBIW watermarking scheme is robust against creative and multiple image attacks, including the puzzle, the kaleidoscope, the kaleidoscope plus tile, the kaleidoscope plus puzzle, and the kaleidoscope plus tile and puzzle attacks.

Table 12 The best extracted watermarks and their Pearson's Correlation Coefficients after Creative Attacks

Creative Attack	FBIW		
	HL	LH	LL&HH
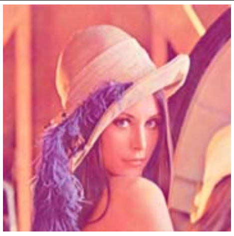			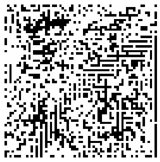
Mosaic: 2	0.8269	0.8273	0.2506
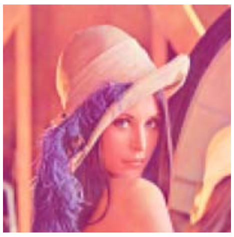	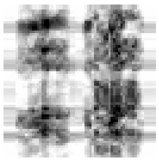	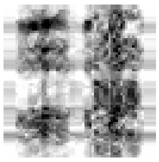	
Mosaic: 5	0.5425	0.4855	0.1008
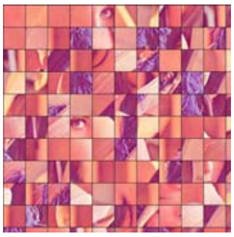			
Puzzle: 50	0.7869	0.7789	0.1920
	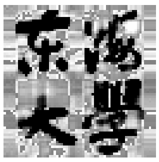	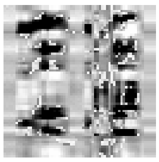	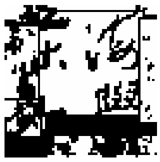
Tile: 50	0.7372	0.6491	0.4113
			
Kaleidoscope Effect	0.0969	0.1931	0.9582

 Kaleidoscope Effect			
	0.2367	0.2143	0.9582
 Kaleidoscope Effect	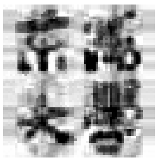		
	0.7280	0.5663	0.9582
 Kaleidoscope Effect + Tile: 50	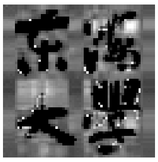	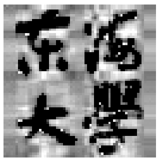	
	0.6564	0.7512	0.1521
 Kaleidoscope Effect + Puzzle: 50	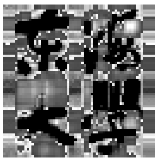	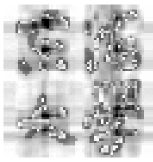	
	0.5823	0.5086	0.1284
 Kaleidoscope Effect + Tile: 50 + Puzzle: 50	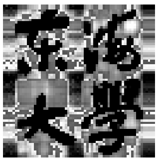	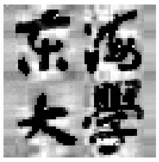	
	0.5973	0.7714	0.1254
 Kaleidoscope Effect + Puzzle 50+ Tile: 50	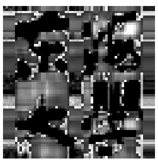	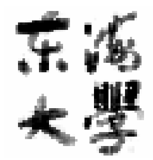	
	0.4809	0.8179	0.1133

3.1.13 Others

We launched other attacks, including the invert, equalize, gama, zoom blur, and resize, on the stego-image to investigate the robustness of the FBIW scheme. The application software is PhotoImpact. We list the experimental results in Table 13. The Pearson's correlation coefficients for the best extracted watermarks are greater than 0.6837. We conclude that the FBIW method is robust against above attacks.

Table 13 The best extracted watermarks and Pearson's Correlation Coefficients after other attacks, including the invert, equalize, gama, zoom blur, and resize.

Other Attacks	FBIW		
	HL	LH	LL&HH
			
Invert	0.8028	0.8029	0.2010
		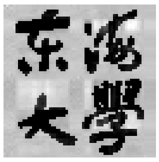	
Equalize	0.8059	0.8036	0.0080
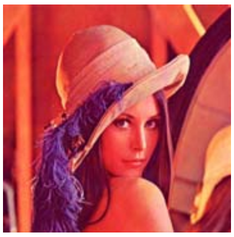	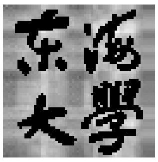	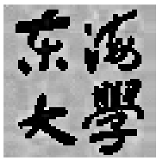	
Gama: 0.5	0.7740	0.7953	0.0121
	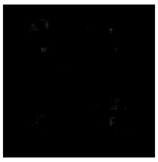		
Zoom Blur: Zoom In: 50	-0.1713	-0.6332	0.9582
			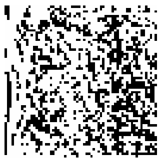
Resized: 256	0.8303	0.8296	0.2380
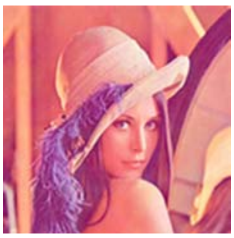	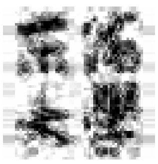		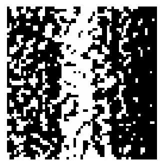
Resize: 128	0.6837	0.6775	0.1209

3.2 RGB Layer Experiment

In this section, we use FBIW method to embed watermark in R, G, B layers and observe the difference among these three layers. We extract the embedded watermarks and list the results in table 14.

- According to the experiment results, if the percentage of the layer is higher in the original image, PSNR value of that layer is higher.
- If the pixel value of each layer is similar, the PSNR will be in the following order: R layer > G layer > B layer.
- If the pixel value of each layer in original image equals to 0, then we cannot extract watermarks from on the LLHH sub-band. The reason is that no information is embedded in the LLHH sub-band by our embedding algorithm at this case.
- When the watermark generates unexpected black blocks, the PSNR of the layer is the highest. The reason is that the no pixel values of stego-image are changed, and so it results in the high PSNR value.

Table 14 The extracting watermark after embedding on R, G, B layers with FBIW

Stego-Image	R		G		B	
	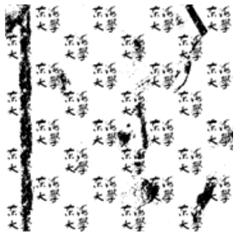					
Corr	0.9562		0.9582		0.9594	
PSNR	LH	HL	LH	HL	LH	HL
R 39.4486 G 39.2793 B 39.0545						
Corr	0.8107	0.8108	0.8029	0.8027	0.7876	0.7875

Stego-Image	R		G		B	
			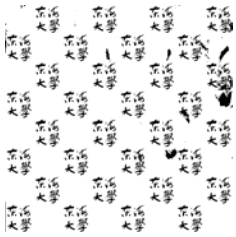			
Corr	0.9562		0.9582		0.9594	
PSNR	LH	HL	LH	HL	LH	HL
R 39.0158 G 39.0767 B 39.0311						
Corr	0.8111	0.8116	0.8026	0.8029	0.7878	0.7877

Stego-Image	R		G		B	
						
Corr	0.9562		0.9582		0.9594	
PSNR	LH	HL	LH	HL	LH	HL
R 40.0542 G 39.2763 B 39.3409						
Corr	0.8110	0.8114	0.8028	0.8028	0.7876	0.7874

Stego-Image	R		G		B	
						
Corr	0.9562		0.9582		0.9594	
PSNR R 39.2527 G 39.3860 B 39.3167	LH 	HL 	LH 	HL 	LH 	HL 
Corr	0.8115	0.8115	0.8027	0.8029	0.7878	0.7878

Stego-Image	R (0)		G (0)		B (0)	
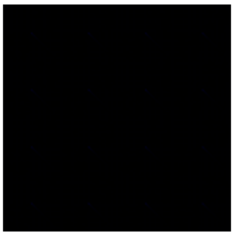						
Corr	0		0		0	
PSNR R 44.2697 G 44.2551 B 44.2477	LH 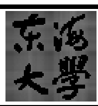	HL 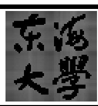	LH 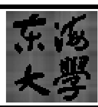	HL 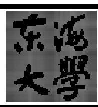	LH 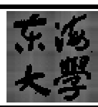	HL 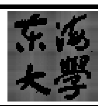
Corr	0.7758	0.7759	0.7898	0.7898	0.7982	0.7982

Stego-Image	R (255)		G (255)		B (255)	
	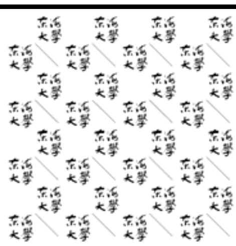		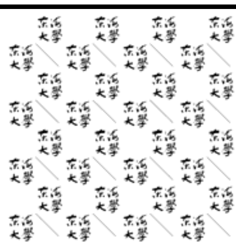			
Corr	0.9562		0.9582		0.9594	
PSNR R 44.8712 G 44.8593 B 44.8339	LH 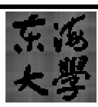	HL 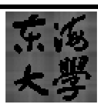	LH 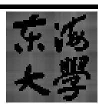	HL 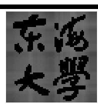	LH 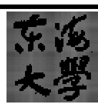	HL 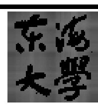
Corr	0.7996	0.8002	0.7915	0.7916	0.7772	0.7775

Stego-Image	R (255)		G (0)		B (255)	
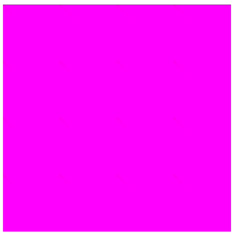						
Corr	0.9562		0		0.9594	
PSNR R 44.8712 G 44.2551 B 44.2815	LH	HL	LH	HL	LH	HL
	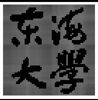	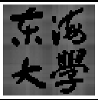	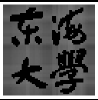	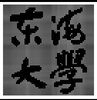	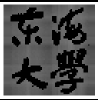	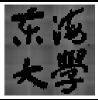
Corr	0.7996	0.8002	0.7898	0.7898	0.7755	0.7730

Stego-Image	R (255)		G (255)		B (0)	
						
Corr	0.9562		0.9582		0	
PSNR R 44.8712 G 44.8593 B 44.2477	LH	HL	LH	HL	LH	HL
	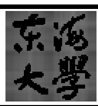	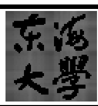	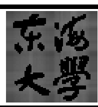	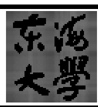	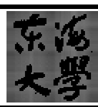	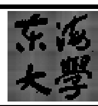
Corr	0.7996	0.8002	0.7915	0.7916	0.7758	0.7759

Stego-Image	R (0)		G (255)		B (255)	
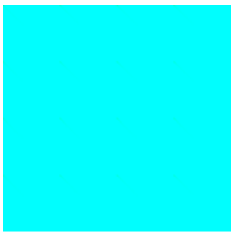			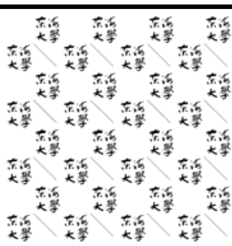		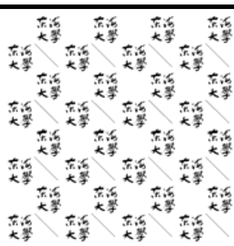	
Corr	0		0.9582		0.9594	
PSNR R 44.2697 G 44.8593 B 44.8339	LH	HL	LH	HL	LH	HL
	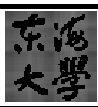	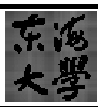	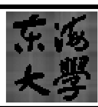	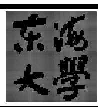	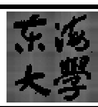	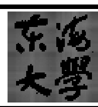
Corr	0.7982	0.7982	0.7915	0.7916	0.7772	0.7775

Stego-Image	R (255)		G (0)		B (0)	
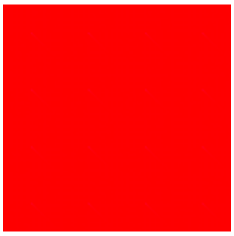						
Corr	0.9562		0		0	
PSNR R 44.3113 G 44.2551 B 44.2477	LH	HL	LH	HL	LH	HL
	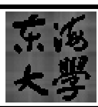	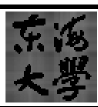	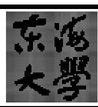	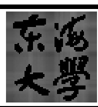	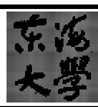	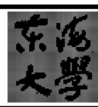
Corr	0.7975	0.7991	0.7898	0.7898	0.7758	0.7759

Stego-Image	R (0)		G (0)		B (255)	
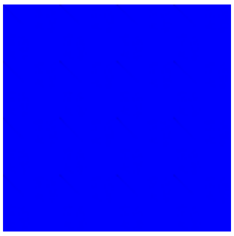						
Corr	0		0		0.9594	
PSNR R 44.2697 G 44.2551 B 44.2815	LH	HL	LH	HL	LH	HL
	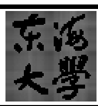	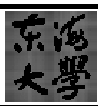	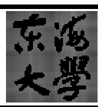	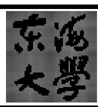	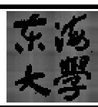	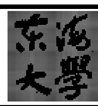
Corr	0.7982	0.7982	0.7898	0.7898	0.7755	0.7760

Stego-Image	R (0)		G (255)		B (0)	
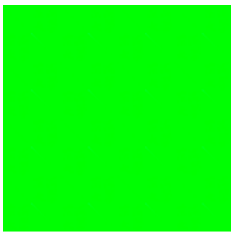			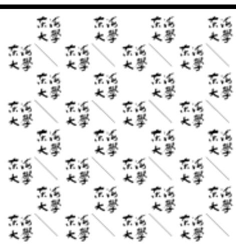			
Corr	0		0.9582		0	
PSNR R 44.2697 G 44.8593 B 44.2477	LH	HL	LH	HL	LH	HL
	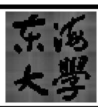	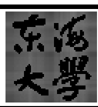	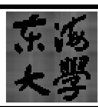	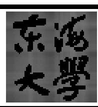	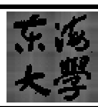	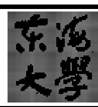
Corr	0.7982	0.7982	0.7915	0.7916	0.7758	0.7759

Stego-Image	R (31)		G (31)		B (31)	
						
Corr	0.9618		0.9582		0.9594	
PSNR R 44.2188 G 44.1009 B 44.0879	LH	HL	LH	HL	LH	HL
	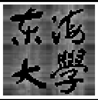		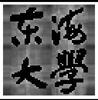	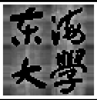	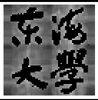	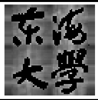
Corr	0.8149	0.8192	0.7268	0.7295	0.7164	0.7182

Stego-Image	R (63)		G (63)		B (63)	
						
Corr	0.9562		0.9582		0.9594	
PSNR R 43.8811 G 43.8681 B 43.8549	LH	HL	LH	HL	LH	HL
	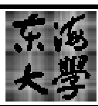	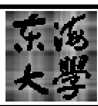	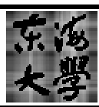	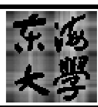		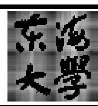
Corr	0.7136	0.7164	0.7071	0.7088	0.6977	0.6987

Stego-Image	R (95)		G (95)		B (95)	
						
Corr	0.9562		0.9582		0.9594	
PSNR R 43.9657 G 43.9424 B 43.9148	LH	HL	LH	HL	LH	HL
	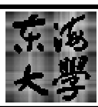	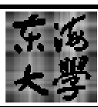	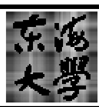	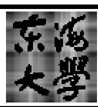	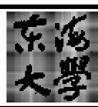	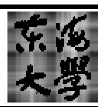
Corr	0.7094	0.7119	0.7028	0.7043	0.6929	0.6941

Stego-Image	R (127)		G (127)		B (127)	
						
Corr	0.9562		0.9582		0.9594	
PSNR R 44.0378 G 44.0141 B 43.9861	LH	HL	LH	HL	LH	HL
	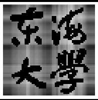	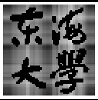	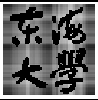	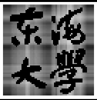	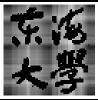	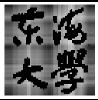
Corr	0.7094	0.7119	0.7028	0.7043	0.6929	0.6941

Stego-Image	R (159)		G (159)		B (159)	
						
Corr	0.9562		0.9582		0.9594	
PSNR R 43.9700 G 43.9467 B 43.9191	LH	HL	LH	HL	LH	HL
	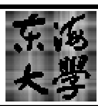	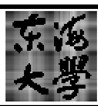	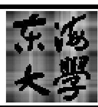	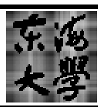		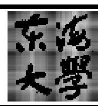
Corr	0.7094	0.7119	0.7028	0.7043	0.6929	0.6941

Stego-Image	R (191)		G (191)		B (191)	
						
Corr	0.9562		0.9582		0.9594	
PSNR R 43.8961 G 43.8832 B 43.8655	LH	HL	LH	HL	LH	HL
	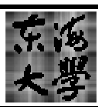	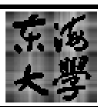	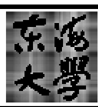	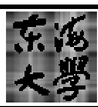	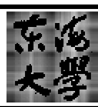	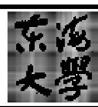
Corr	0.7137	0.7165	0.7073	0.7090	0.6981	0.6981

Stego-Image	R (223)		G (223)		B (223)	
						
Corr	0.9562		0.9582		0.9594	
PSNR R 44.1498 G 44.1393 B 44.1166	LH	HL	LH	HL	LH	HL
	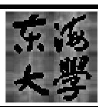	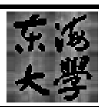	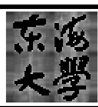	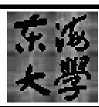	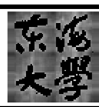	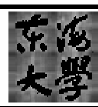
Corr	0.7343	0.7367	0.7274	0.7290	0.7169	0.7177

Chapter 4
Second Form of FBIW

4.1 Embedding and Extracting Algorithms of the Second Form of FBIW

The watermarks are embedded in the HL and LH sub-bands by the SVD method and in the HH and LL sub-bands by the DDWT method in the previous FBIW method. We investigate the effectiveness and robustness of the FBIW method by embedding watermarks in the second form, that is, we embed watermarks in the HH and LL sub-bands by the SVD method and in the HL and LH sub-bands by the DDWT method. We find that the stego-image of the second form of FBIW has higher PSNR value and the second form is more robust than the first form.

The embedding algorithm and extracted algorithm of the second form of the FBIW method is described below:

4.1.1 Embedding algorithm of the second form

Step 1: Input the original image X ($M\times M$) and the watermark W ($N\times N$).

Step 2: Perform the K-scale DDWT transform on X to obtain X', where K is the number of scale.

(Step 3 to Step 6 embedding the watermark in HH and LL sub-bands utilizing the SVD method)

Step 3: Set initial values of the stego-image in the frequency domain Y' to be equal to X', and apply SVD on sub-bands HH and LL of the last scale:

$$X'^{HH} = U_{X'}^{HH} \sum_{X'}^{HH} V_{X'}^{HHT} \tag{15}$$

$$X'^{LL} = U_{X'}^{LL} \sum_{X'}^{LL} V_{X'}^{LLT}$$

Where X'^{HH} and X'^{LL} represent X' in sub-bands *HH* and *LL*, and the diagonal elements ($\sigma_{X'i}^{HH}$ and $\sigma_{X'i}^{LL}$) of $\sum_{X'}^{HH}$ and $\sum_{X'}^{LL}$ are the singular values on sub-bands HH and LL. The singular values on sub-bands HH and LL must satisfy $\sigma_{X'1}^{HH} \geq \sigma_{X'2}^{HH} \geq \cdots \geq \sigma_{X'M}^{HH} \geq 0$ and $\sigma_{X'1}^{LL} \geq \sigma_{X'2}^{LL} \geq \cdots \geq \sigma_{X'M}^{LL} \geq 0$.

Step 4: Apply SVD to the watermark:

$$W = U_W \Sigma_W V_W^T \tag{16}$$

Where the diagonal elements (σ_{Wi}) of Σ_W are the singular values of the watermark, and $\sigma_W = [\sigma_{W1}, \sigma_{W2}, \cdots, \sigma_{WN}]$, $\sigma_{W1} \geq \sigma_{W2} \geq \cdots \geq \sigma_{WN} \geq 0$

Step 5: Process the singular values of X' in the frequency domain with the singular values of the watermark:

$$\sigma_Y^{HH} = \sigma_{X'}^{HH} + \alpha_i \sigma_{Wi} \tag{17}$$

$$\sigma_Y^{LL} = \sigma_{X'}^{LL} + \alpha_i \sigma_{Wi}$$

Where i=1, 2, ..., N and setting the value of α_i, α is a scaling factor. It will affect the quality of embedded watermark and $\sigma_{Y'}$ is the singular values of the singular matrix $\Sigma Y'$.

Step 6: Obtain Y'^{HH} and Y'^{LL} embedded with watermarks on sub-bands *HH* and *LL*:

$$Y^{HH} = U_{X'}^{HH} \sum_{Y}^{HH} V_{X'}^{HHT} \tag{18}$$

$$Y^{LL} = U_{X'}^{LL} \sum_{Y}^{LL} V_{X'}^{LLT}$$

Step 7: Take Y'^{HH} and Y'^{LL} of the last scale of Y' and perform inverse DDWT to obtain spatial domain Y_{HHLL} that has been embedded with watermarks in sub-bands *HH* and *LL*.

(Step 8 embedding the watermark in sub-bands *LH* and *HL* utilizing the DDWT method)

Step 8: Take Y' data in the sub-bands *LH* and *HL* of the last scale and embed watermark information according to the following formula:

$$\begin{aligned} &If\ W_{ij} = 0\ then\ Y_{ij}^{LH} = Y_{ij}^{LH} + (2^K)^2 \times \alpha \\ &If\ W_{ij} = 1\ then\ Y_{ij}^{HL} = Y_{ij}^{HL} + (2^K)^2 \times \alpha \end{aligned} \tag{19}$$

Step 9: Apply the inverse DDWT to Y' to produce the stego-image Y, which has been embedded with watermark information on the four sub-bands of the last scale. Subtract Y_{HHLL} from Y to obtain Y_{Diff}, which gives difference of pixel values of Y_{HHLL} and Y in the spatial domain.

4.1.2 Extracting algorithm

(Step 1 to Step 2 extracting the watermark from sub-bands *LH* and *HL*)

Step 1: Input the stego-image Y, the original image X, the spatial domain data Y_{HHLL}, and the watermark W.

Step 2: Subtract Y_{HHLL} from Y to obtain Y_{LHHL}, and apply formula (20) on Y_{LHHL} to extract the embedded watermark W^{LHHL}:

$$W_{ij}^{LHHL} \begin{cases} = 0 & if\ E_{LHHL} < 0 \\ = 1 & otherwise \end{cases} \tag{20}$$

(Step 3 to Step 6 extracting the watermark from sub-bands *HH* and *LL*)

Step 3: Subtract Y_{Diff} from Y to obtain F, and then apply the multi-scale DDWT on F to obtain F'.

Step 4: Apply SVD to F' on sub-bands *HH* and *LL* of the last scale:

$$F'^{HH} = U_{F'}^{HH} \sum_{F'}^{HH} V_{F'}^{HHT} \tag{21}$$
$$F'^{LL} = U_{F'}^{LL} \sum_{F'}^{LL} V_{F'}^{LLT}$$

Where F'^{HH} and F'^{LL} represent F' in the sub-bands *HH* and *LL* of the last scale, and the diagonal elements ($\sigma_{F'}^{HH}$ and $\sigma_{F'}^{LL}$) of $\Sigma_{F'}^{HH}$ and $\Sigma_{F'}^{LL}$ are the singular values of F'^{HH} and F'^{LL}.

Step 5: Extract the singular values of watermarks by processing the diagonal elements of $\Sigma_{F'}^{HH}$ with $\Sigma_{X'}^{HH}$ and $\Sigma_{F'}^{LL}$ with $\Sigma_{X'}^{LL}$, respectively.

$$\sigma_W^{HH} = \frac{\sigma_{F'}^{HH} - \sigma_{X'}^{HH}}{\alpha_i} \tag{22}$$
$$\sigma_W^{LL} = \frac{\sigma_{F'}^{LL} - \sigma_{X'}^{LL}}{\alpha_i}$$

Where i = 1, 2… N. σ_W^{HH} and σ_W^{LL} is extracting SVD from HH and LL.

Step 6: Obtain the two watermarks embedded in sub-bands *HH* and *LL* by the following equations:

$$W^{HH} = U_W^{HH} \sum_W^{HH} V_W^T \tag{23}$$
$$W^{LL} = U_W^{LL} \sum_W^{LL} V_W^T$$

4.2 Experimental Results of Second Form

The original cover image Lena (512 × 512) is shown in Fig. 3(a), and the watermark (64 × 64), in Fig. 3(b) in Chapter 3. We embedded watermarks in the full band of the cover image after doing 3-scale DDWT. The intension (α) of watermark in each sub-band is 1. The stego-image Lena is shown in fig. 5(a). The watermarks extracted from sub-bands HL& LH are shown in Fig. 5(b). The watermarks extracted from sub-bands HH and LL are shown in Fig. 5(c) and Fig. 5(d), respectively. The PSNR value of the second form of FBIW method is slightly higher than the PSNR value of the first form as shown in Table 15.

Table 15 PSNR of stego-image of first and second forms of FBIW in RGB layer.

	Second Form	First Form
R	39.9662	39.4486
G	39.3339	39.2793
B	39.4610	39.0545

(a) (b) (c) (d)

Fig. 6 (a) The stego-image Lena (PSNR=39.3339)
(b) The extracted watermark from sub-bands LH&HL (Corr=0.9582)
(c) The extracted watermark from the sub-band HH (Corr=0.8027)
(d) The extracted watermark from the sub-band LL (Corr=0.8007).

4.3 Image Attacking Experiment on the Second Form of FBIW

Table 16 shows parameters, attacked image and software used of attacks on the stego-image with watermarks embedded by the second form of the FBIW method. Eighteen attacks are used, including the croppings (cropping on both sides, cropping 50%, cropping 7%, cropping 85%, cropping 95%), contrast adjustments (adjustment -20, 40, 60, and 80), rotations (rotate angle 20° and 45°), Gamma blur, histogram equalization, sharpening, Gaussian correction, pixelate, rescaling and Gaussian noises.

Table 16 Testing attacks, parameters, attacked image and software used, on the stego-image embedded by the second form of FBIW

Attacks	Crop on both sides	Crop 50	Crop 70	Crop 85
Parameters	Crop on both of image sides	Crop 50% area	Crop 70% area	Crop 85% area
Attacked image		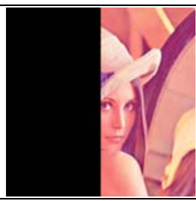	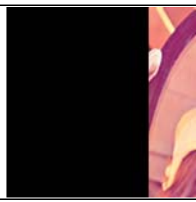	
Software	Photoimpact	Photoimpact	Photoimpact	Photoimpact
Attacks	Crop 95	Contrast -20	Contrast 40	Contrast 60
Parameters	Crop 95% area	Contrast adjustment -20	Contrast adjustment 40	Contrast adjustment 60
Attacked image	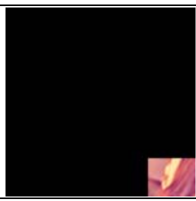	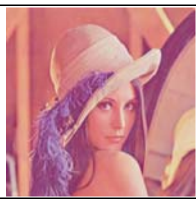	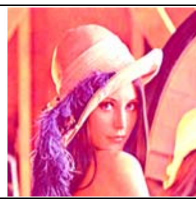	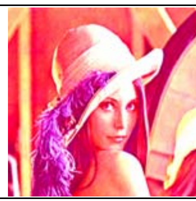
Software	Photoimpact	Photoimpact	Photoimpact	Photoimpact
Attacks	Contrast 80	Rotation 20°	Rotation 45°	Gaussian Blur
Parameters	Contrast adjustment 80	Rotate angle 20°	Rotate angle 45°	5x5
Attacked image				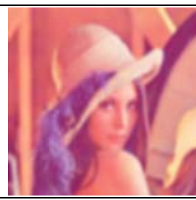
Software	Photoimpact	Photoimpact	Photoimpact	Photoimpact
Attacks	Histogram equalization	Sharpening	Gamma correction	Pixelate
Parameters	Auto-level	Sharpen 80	0.5	mosaic 2 pixels
Attacked image			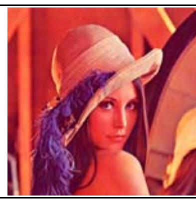	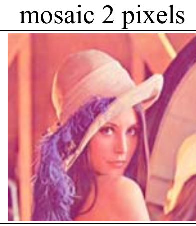
Software	Photoimpact	Photoshop	Photoimpact	Photoimpact
Attacks	Rescale	Gaussian noise	—	—
Parameters	512→256→512	0.3	—	—
Attacked image	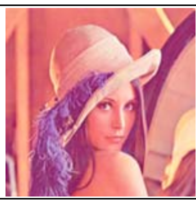	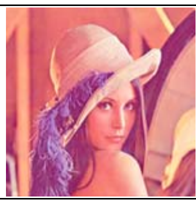	—	—
Software	Photoimpact	Photoshop	—	—

Table 17 shows the best extracted watermarks and their Pearson's correlation coefficients by using the first form and the second form of the FBIW methods. The value of the Pearson's correlation coefficient is shown under each extracted watermark. The first form of FBIW extracts three kinds of watermarks from sub-bands LL&HH, sub-band HL and sub-band LH. Likewise, the second form of FBIW extracts three kinds of watermarks from sub-bands LH& HL, sub-band HH and sub-band LL. Considering that we can always choose the best one from all the extracted watermarks to claim copyright, we will compare the second form with the first form by the best extracted watermark as shown in Table 17.

From Table 17, we observe that the second form is as robust as the first form against cropping and rotation attacks, and the second form is more robust than the first form against other attacks. Table 18 shows the above observation, and cups, showing as, are given to the method with the best value of Pearson's Correlation Coefficient.

Table 17 The best extracted watermarks and their Pearson's Correlation Coefficient value of the first and second form of FBIW methods

Attacks	**First Form**	**First Form**	**First Form**	**Second Form**	**Second form**	**Second Form**
Crop on both sides		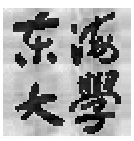	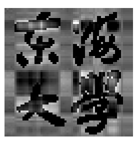		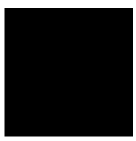	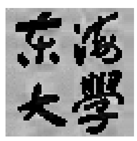
Corr(W,W')	0.9582	0.7785	0.5749	0.9582	-	0.8321
Sub-band	LLHH	HL	LH	HLLH	LL	HH
Crop 50		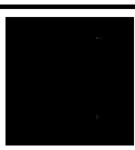				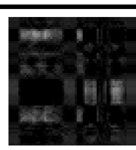
Corr(W,W')	0.9582	-0.0333	-0.6457	0.9582	-	-0.3880
Sub-band	LLHH	HL	LH	HLLH	LL	HH

Crop 70	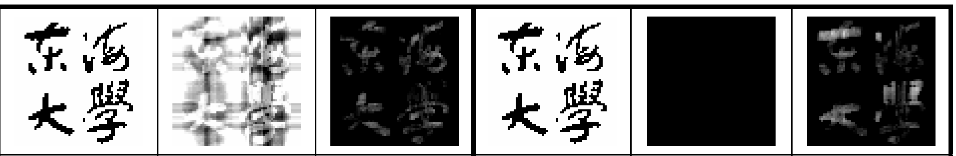					
Corr(*W*,*W'*)	0.9582	-0.1655	-0.6338	0.9582	-	-0.7025
Sub-band	LLHH	HL	LH	HLLH	LL	HH
Crop 85	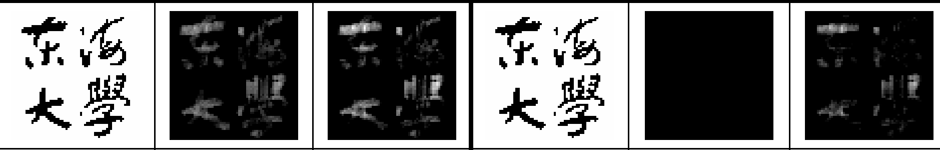					
Corr(*W*,*W'*)	0.9582	-0.7224	-0.6481	0.9582	-	-0.5420
Sub-band	LLHH	HL	LH	HLLH	LL	HH
Crop 95	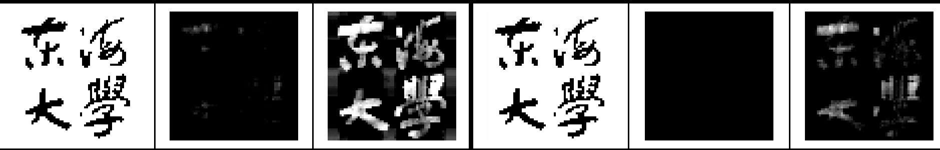					
Corr(*W*,*W'*)	0.9582	-0.3271	-0.7683	0.9582	-	-0.6505
Sub-band	LLHH	HL	LH	HLLH	LL	HH
Contrast -20	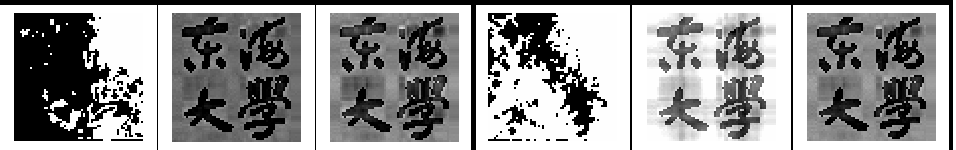					
Corr(*W*,*W'*)	0.3003	0.7694	0.7094	0.3705	0.7654	0.7849
Sub-band	LLHH	HL	LH	HLLH	LL	HH
Contrast 40	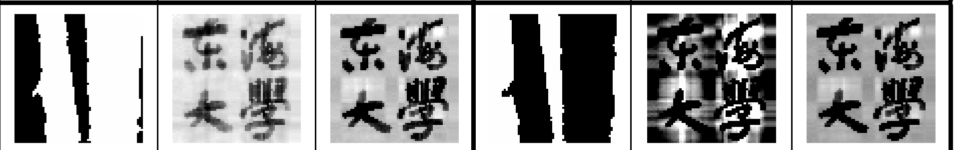					
Corr(*W*,*W'*)	0.1893	0.8125	0.8104	0.2111	0.4623	0.8293
Sub-band	LLHH	HL	LH	HLLH	LL	HH
Contrast 60						
Corr(*W*,*W'*)	0.1939	0.4141	0.7885	0.2079	0.4303	0.8178
Sub-band	LLHH	HL	LH	HLLH	LL	HH
Contrast 80	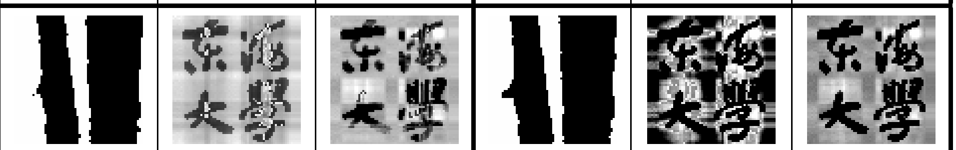					
Corr(*W*,*W'*)	0.1982	0.6325	0.7563	0.2056	0.4810	0.8029
Sub-band	LLHH	HL	LH	HLLH	LL	HH

Rotation 20°	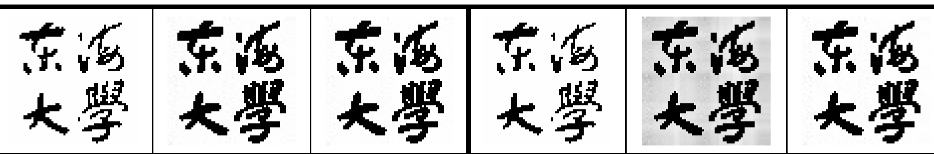					
Corr(W,W')	0.9582	0.8027	0.8029	0.9582	0.8370	0.8392
Sub-band	LLHH	HL	LH	HLLH	LL	HH
Rotation 45°	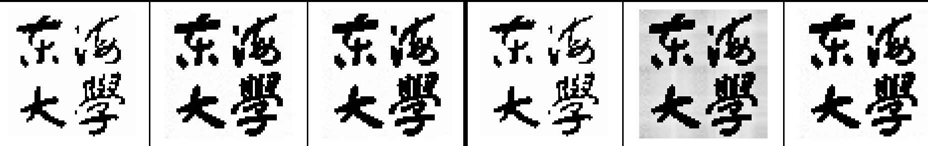					
Corr(W,W')	0.9582	0.8027	0.8029	0.9582	0.8370	0.8392
Sub-band	LLHH	HL	LH	HLLH	LL	HH
Gaussian Blur	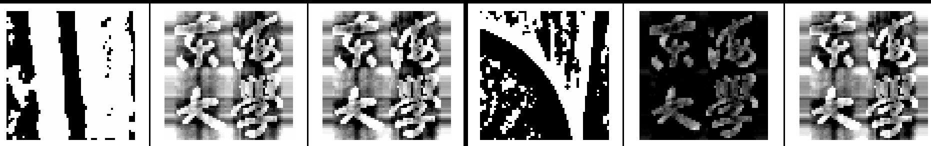					
Corr(W,W')	0.1592	-0.3430	-0.3869	0.1601	-0.7109	-0.3707
Sub-band	LLHH	HL	LH	HLLH	LL	HH
Histogram equalization	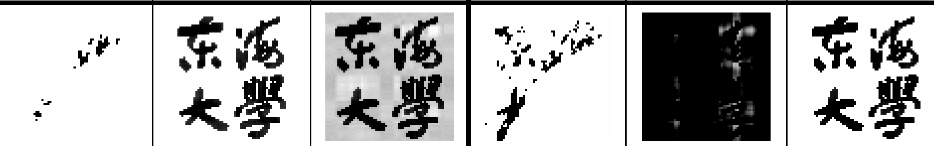					
Corr(W,W')	0.2143	0.8164	0.8050	0.4075	0.1271	0.8434
Sub-band	LLHH	HL	LH	HLLH	LL	HH
Sharpening	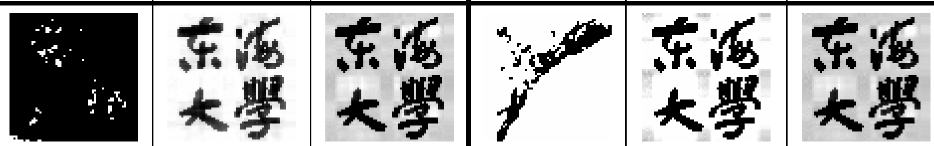					
Corr(W,W')	0.2898	0.8220	0.8030	0.2609	0.8359	0.8398
Sub-band	LLHH	HL	LH	HLLH	LL	HH
Gamma correction	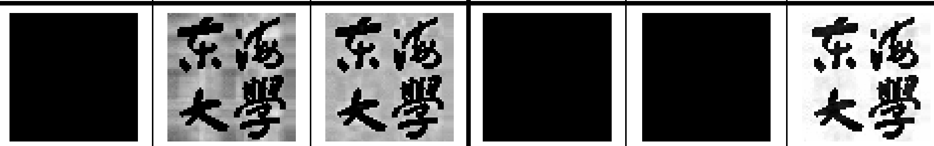					
Corr(W,W')	0.0121	0.7740	0.7953	0.0353	-	0.8332
Sub-band	LLHH	HL	LH	HLLH	LL	HH
Pixelate						
Corr(W,W')	0.2506	0.8269	0.8273	0.2489	0.8367	0.8611
Sub-band	LLHH	HL	LH	HLLH	LL	HH

Rescale						
Corr(W,W')	0.2380	0.8303	0.8296	0.2467	0.8533	0.8551
Sub-band	LLHH	HL	LH	HLLH	LL	HH
Gaussian noise					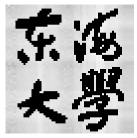	
Corr(W,W')	0.7817	0.8027	0.8028	0.7824	0.8368	0.8392
Sub-band	LLHH	HL	LH	HLLH	LL	HH

Table 18 Comparison of the first and second forms of FBIW methods under all attacks

Attacks	The Second Form	The First Form
Cropping	🏆	🏆
Contrast adjustment	🏆	
Rotation	🏆	🏆
Gamma correction	🏆	
Gaussian blur	🏆	
Histogram equalization	🏆	
Sharpening	🏆	
Rescaling	🏆	
Pixelate	🏆	
Gaussian noise	🏆	

Chapter 5
Conclusions

An effective digital watermarking scheme needs to be invisible as well as robust. The FBIW scheme is very effective, that is, it has high PSNR value for the stego-image, and is robust against common geometric and non-geometric attacks.

New image attacks come along with new and efficient image processing tools. To evaluate the security of the FBIW scheme against new attacks, we test on the stego-image with a wide range of attacks, destructive or creative, single or multiple ones. Experimental results show that FBIW is not only very robust against most image attacks, such as rotation, cropping, the ripple, and the whirlpool attacks, but also very robust against creative and multiple image attacks, such as the kaleidoscope plus tile, the kaleidoscope plus puzzle, and the kaleidoscope plus tile and puzzle attacks. The FBIW scheme combines merits of DDWT and SVD watermarking techniques and is proved to be very secure against image attacks.

In new era of information technology, internet has become the main gateway to seek recreations, promote commercial products, and perform business deals. In order to ban unauthorized reproductions and distribution of multimedia files (e.g. videos, songs and images), researchers develop various digital watermarking techniques to protect digital rights of every internet user. The DDWT method is robust against the cropping attack but it is vulnerable to geometric attacks (e.g. rotation, scaling or transposition) or non-geometric attacks (e.g. contrast adjustment, sharpen and histogram equalization).

DDWT technique transforms original image data from the spatial domain into the frequency domain. The stego-image has high Peak Signal to Noise Ratio (PSNR) value when we apply the DDWT watermarking embedding process; however, it is vulnerable to various attacks. The FBIW method, which is developed from DDWT and SVD schemes, produces high quality stego-image and the embedded watermark has high resistance against a variety of common geometric and non-geometric attacks.

The best digital watermarking scheme achieves the goals of superior information hiding and embedded data should be immune to various image attacks. Watermark information is embedded invisibly in digital images and is extracted to defend the ownership of digital multimedia and preserve the legal owner's right and interest. The visual quality of extracted watermarks and corresponding correlation coefficients of them indicate the robustness of the FBIW watermarking scheme. It is very robust against many attacks, such as the Gaussian noise, sharpening, the histogram equalization, rotation, cropping, warm, the ripple, the whirlpool, the crystal and glass, the blast, the watercolor, the colored pen, mosaic, the invert, equalization, Gamma, the zoom blur, the resizing attacks. It also shows good robustness against other attacks.

Experiments on RGB layers show that embedded information will be more invisible when we embed watermark image into color layer having the highest RGB values. When the pixels of RGB layers are equal, the R layer is the most priority layer to choose from; then the G layer and finally the B layer. When the embedded watermark fails to be extracted, the digital watermarking scheme is invalid.

PSNR values of embedded watermarks vary from different watermarking schemes and it influences the performance of extracted watermarks. Stego-image processed by the second form of FBIW method has higher PSNR values than the first form of FBIW method. Experimental results demonstrate that stego-image processed by the second form of the FBIW method is more robust than the first form since it has higher Pearson's correlation coefficients.

Bibliography

[1] A. Munteanu, J. Cornelis, G. Van der Auwera and P. Cristea, "Wavelet Image Compression - The Quadtree Coding Approach," *IEEE Trans. on Information Technology in Biomedicine*, Vol. 3, Sept., 1999, pp. 176-185.

[2] C. H. Lin, J. C. Liu and P. C. Han, "On the Security of the Full-Band Image Watermark," *IEEE International Conference on Sensor Networks, Ubiquitous, and Trustworthy Computing (SUTC2008)*, June 11-13 2008, pp. 74-80.

[3] C. H. Lin, J. S. Jen and L. C. Kuo, "Distributed Discrete Wavelet Transformation for Copyright Protection," *7th International Workshop on Image Analysis for Multimedia Interactive Services (WIAMIS 2006)*, April 19-21 2006, pp. 53-56.

[4] C. Y. Lin, M. Wu, J. A. Bloom, I. J. Cox, M. L. Miller, and Y.M. Lui, "Rotation , Scale and Translation resilient watermarking for images," *IEEE Transactions on Image Processing*, vol. 10, no. 5, 2001.

[5] Chandra, D.V.S., "Digital image watermarking using singular value decomposition," *The 45th Midwest Symposium on Circuits and Systems(MWSCAS-2002)* Vol.3, Aug. 2002, pp. III-264 - III-267

[6] Craizer, M., Silva, E. A. B. D. and Ramos, E. G., "Convergent algorithms for successive approximation vector quantization with applications to wavelet image compression," *IEE Proceedings-Vision Image and Signal Processing*, Vol. 146, No.3, Jun. 1999, pp. 159-164.

[7] D. P. O'Leary and S. Peleg, "Digital Image Compression by Outer Product Expansion," *IEEE Transactions on Communications*, March 1983, pp. 441-444.

[8] H. C. Andrews and C. L. Patterson, "Singular Value Decomposition (SVD) Image Coding," *IEEE Transactions on Communications*, April 1976, pp. 425-432.

[9] J. C. Liu, C. H. Lin, and L. C. Kuo. "A Robust Full-Band Image Watermarking Scheme," *Communication systems, 2006. ICCS 2006. 10th IEEE Singapore International Conference*, Oct. 2006, pp. 1-5.

[10] J. C. Liu, C. H. Lin, L. C. Kuo, and J. C. Chang, "Robust Multi-scale Full-band Image Watermarking for Copyright Protection," *The 20th International Conference on Industrial, Engineering and Other Applications of Applied Intelligent Systems (IEA/AIE 2007)*, LNAI 4570, June 26-29 2007, Kyoto, Japan, pp. 175-183.

[11] J. S. Tsai, W. B. Huang, C. L. Chen, and Y. H. Kuo, "A Feature-Based Digital Image Watermarking for Copyright Protection and Content Authentication," *Image Processing, ICIP 2007. IEEE International Conference,* Sept. 16 2007-Oct. 19 2007, San Antonio, TX, pp. 469-472.

[12] J. F. Yang and C. L. Lu, "Combined Techniques of Singular Value Decomposition and Vector Quantization," *IEEE Transactions on Image Processing*, August 1995, pp. 1141-1146.

[13] J. Lee, and C. S. Won, "A Watermarking Sequence Using Parities of Error Control Coding for Image Authentication and Correction," *IEEE Transactions on Consumer Electronics*, vol. 46, no. 2, pp. 313-317, 2000.

[14] J.M. Shapiro, "Embedded image coding using zerotrees of wavelet coefficients," *IEEE Trans. Signal Processing*, Vol. 41, Dec. 1993, pp. 3445-3463.

[15] K. Konstantinides and G. S. Yovanof, "Application of SVD-Based Spatial Filtering to Video Sequences," *IEEE International Conference on Acoustics, Speech and Signal Processing*, Vol. 4, Detroit, MI, May 9-12, 1995, pp. 2193-2196.

[16] K. Konstantinides and G. S. Yovanof, "Improved Compression Performance Using SVD-Based Filters for Still Images," *SPIE Proceedings*, Vol. 2418, San Jose, CA, February 7-8, 1995, pp. 100-106.

[17] K. Konstantinides, B. Natarajan and G. S. Yovanof, "Noise Estimation and Filtering Using Block-Based Singular Value Decomposition," *IEEE Transactions on Image Processing*, March 1997, pp. 479-483.

[18] M. Antonini, M. Barlaud, P. Mathieu and I. Daubechies, "Image Coding Using Wavelet Transform," *IEEE Trans on Image Processing*, Vol.1,No.2, April 1992, pp. 205-220.

[19] N. Garguir, "Comparative Performance of SVD and Adaptive Cosine Transform in Coding Images," *IEEE Transactions on Communications*, August 1979, pp. 1230-1234.

[20] P. Waldemar and T. A. Ramstad, "Hybrid KLT-SVD Image Compression," *IEEE International Conference on Acoustics, Speech and Signal Processing*, Vol. 4, Munich, Germany, April 21-24, 1997, pp. 2713-2716.

[21] R. Karkarala and P. O. Ogunbona, "Signal Analysis Using a Multiresolution Form of the Singular Value Decomposition," *IEEE Transactions on Image Processing*, May 2001, pp. 724-735.

[22] Ruizhen Liu and Tieniu Tan, "An SVD-based watermarking scheme for protecting rightful ownership," *IEEE Transactions on Multimedia*, Vol.4, Issue1, March 2002, pp. 121-128.

[23] S. D. Lin, and C. F. Chen, "A Robust Dct-based Watermarking for Copyright Protection," *IEEE Transaction on Consumer Electronics*, Vol. 46, No. 3, August 2000, pp. 415-421.

[24] S. O. Aase, J. H. Husoy and P. Waldemar, "A Critique of SVD-Based Image Coding Systems," *IEEE International Symposium on Circuits and Systems VLSI*, Vol. 4, Orlando, FL, May 1999, pp. 13-16.

[25] S.G. Mallat, "A Theory for Multiresolution Signal Decomposition: The Wavelet Representation," *IEEE Trans. on PAMI*, Vol. 11,No.7, July 1989, pp. 674-693.